



Magnetic and chemical biomonitoring of particulate matter at cultural heritage sites: The Peggy Guggenheim Collection case study (Venice, Italy)

Lisa Grifoni^{a,b}, Aldo Winkler^{b,*}, Luigi Antonello Di Lella^a, Luciano Pensabene Buemi^c, Antonio Sgamellotti^d, Lilla Spagnuolo^b, Stefano Loppi^a

^a Department of Life Sciences, University of Siena, Siena 53100, Italy

^b Istituto Nazionale di Geofisica e Vulcanologia, Rome 00143, Italy

^c Peggy Guggenheim Collection, Venice 30123, Italy

^d Accademia Nazionale dei Lincei, Rome 00165, Italy

ARTICLE INFO

Keywords:

Magnetic biomonitoring
Particulate matter
Lichens
Cultural heritage
Preventive conservation
Trace metals

ABSTRACT

Cultural heritage (CH) is heavily threatened by air pollution, especially by airborne particulate matter (PM), that acts on the surfaces of fine arts, causing artistic loss. Therefore, the monitoring of air quality assumes a central role for the preventive conservation of CH.

In this study, magnetic and chemical biomonitoring of PM was applied at the Peggy Guggenheim Collection, a contemporary and modern art museum in Venice, Italy. It is located in an aquatic context, where the PM sources are considerably different, with respect to the usual vehicular-dominated urban emissions.

Lichen biomonitoring is a well-established technique for the assessment of air quality, especially where PM collecting devices cannot be operated for aesthetic and practical reasons.

Samples of the lichen species *Evernia prunastri* were collected from a pristine area and exposed for three months (November 2022–February 2023) at increasing distances from the Grand Canal, planning an outdoor vs. indoor sampling design, for outlining the diffusion of airborne PM inside the museum.

In combination with lichen exposure, the leaves of *Pittosporum tobira* hedges were sampled for determining their efficiency as bioaccumulators.

The magnetic properties of lichens showed a moderate bioaccumulation of magnetite-like particles outdoors. Conversely, the magnetic properties of the indoor samples were like those of the unexposed ones, indicating a negligible accumulation of metallic particles indoors. *Pittosporum tobira* leaves mostly showed diamagnetic properties, resulting an ineffective species for preventing conservation purposes. Chemical analysis did not show any significant difference between unexposed, indoor and outdoor samples. A directional gradient of bioaccumulation was not evident, thus implying that the sources of metallic PM are distant or diffused, with respect to the site.

The joint use of magnetic and chemical analyses was useful for evaluating the negligible impact of airborne particulate pollution arising from the Grand Canal towards the Halls of the Collection.

1. Introduction

Biomonitoring of particulate matter (PM) applied to cultural heritage is an innovative strategy of preventive conservation from damage caused by this airborne pollutant. Atmospheric PM is one of the main causes of degradation of fine arts, damaging their surfaces by different chemical-physical processes (Comite et al., 2019).

Historical buildings in urban settlements are directly exposed to

airborne pollutants that create “soiling” or “black crusts”, derived from airborne particles deposited on monuments, paintings and masterpieces, generating a thick coating that alters their surfaces and compromises their maintenance. Paintings, frescoes and statues are exposed to damage even if inside a museum. This is because PM can enter or be resuspended by multiple factors, for instance: the air flowing from the conditioning systems, the doors and windows, or the passage of visitors through the rooms. The International Centre for the Study of the

* Corresponding author.

E-mail address: aldo.winkler@ingv.it (A. Winkler).

<https://doi.org/10.1016/j.envadv.2023.100455>

Preservation and Restoration of Cultural Property (ICCROM) promotes preventive conservation as a valid instrument against the deterioration of fine arts. In urban contexts, where cultural heritage sites are predominantly located, common sources of these particles are fuel combustion, vehicle brake wearing, industrial activities, heating systems and natural sources, such as wind-blown dusts. This ensemble of particles, widespread in the atmosphere, may contain magnetite-like particles of different grain sizes and magnetic properties, that are mainly connected with anthropogenic activities, especially in trafficked urban areas, where they mainly derive from emission sources like brake abrasion, or iron oxides produced during combustion processes (Hunt et al., 1984; Georgeaud, 1997; Maher et al., 2008; Gonet et al., 2021a, 2021b; Winkler et al., 2020). The use of biomonitors such as mosses (Salo, 2014; Salo and Mäkinen, 2019) lichens and plant leaves is a well-known and widespread technique of air monitoring, owing to the efficacy of these organisms in accumulating even very high loads of airborne anthropogenic particles that in urban areas are enriched in potentially toxic elements (PTEs) such as Fe, Cr, Cu, Sb, Al, Zn, Ba, etc. Biomonitors act as a cost-effective control unit, easy to handle, offering an estimation of air quality in a specific area. Moreover, the use of lichen transplants collected in a remote environment and exposed in the site of interest provides a detailed estimation of the deposition of pollutants over a well-defined time period and knowing the starting composition.

The use of lichen transplants offers the further possibility to expose the same biomonitors both outdoors and indoors, considering their successful applications in several indoor case studies too (e.g.: Canha et al. 2014; Protano et al. 2017; Almeida et al. 2011; Paoli et al., 2019).

These biomonitors are particularly suitable for the estimation of pollutants close to monuments, museums, or archaeological sites because the exposure of lichen transplants is readily feasible, not easily visible and the risk of biological contamination is minimal. Moreover, lichen and leaves are very effective for providing experimental high spatial resolution monitoring designs that are not feasible using conventional automated air quality devices. Indeed, biomonitoring gives a different perspective with respect to other methods to assess air pollution, such as modeling based on emission data or measurements of ambient air concentrations of pollutants, providing original parameters based on their biological response and the possible biological effects of harmful emissions.

Magnetic biomonitoring techniques provide a proxy for the anthropogenic fraction of PM, that is often linked to the presence of iron oxides, which are well characterizable in terms of composition, concentration and grain-size distribution (Hofman et al., 2017; Chaparro, 2021).

The first study about magnetic biomonitoring concerning cultural heritage preventive conservation was drawn at Villa Farnesina, located in a busy area of Rome, where PM distribution from the main street towards the frescoed Lodges was assessed through magnetic and chemical analyses on lichens and leaves (Winkler et al., 2022). Lichens demonstrated to be the best biomonitors, while leaves are worth to be investigated for their PM retention properties and the consequent provision of ecosystem services.

This study focuses on the Peggy Guggenheim Collection, a prestigious cultural heritage setting inside the UNESCO World Heritage site of Venice, Italy. Chemical and magnetic analyses were applied to lichens exposed for three months inside and outside the halls of the Collection, with the aim of assessing the impact of outdoor airborne PM on the indoor artworks. Leaves of *Pittosporum tobira* hedges were also collected and subjected to magnetic analysis to characterise the metallic emissions arising from the Grand Canal (the main route of transportation in Venice) towards the Museum's halls, as well as to evaluate the possible use of this plant species for the removal of anthropogenic PM.

2. Materials and methods

2.1. Study area

The Peggy Guggenheim Collection is located in the Venier dei Leoni Palace, along the Grand Canal, in the city centre of Venice. This building was projected in 1749 by the architect Lorenzo Boschetti, and it was inhabited by many families until 1949, when Peggy Guggenheim decided to live there. She was an important American art collector, and her collection hosts masterpieces by Magritte, Picasso, Pollock, Ernst and many other contemporary artists. She decided to open her remarkable collection to the public in 1951, and since then it has been visited by millions of visitors.

The historical building, expected to be on 3 floors and not completed, is based on the ground floor only with a big terrace facing the Grand Canal and a rooftop garden. On the opposite side, the palace has a suggestive garden with trees of the species *Cupressus sempervirens*, *Cladastris lutea*, *Tilia americana* and *Betula nigra* and many other plants in hedges and flowerbeds. Hedges of *Pittosporum tobira* figure the railings in the terrace on the Grand Canal and the rooftop garden as well as the entrance in the building from the garden: thus, *P. tobira* is the only ubiquitous plant species available all around the museum.

2.2. Lichen exposure

The lichen *Evernia prunastri* (L.) Ach. was the biomonitor selected according to its suitability in environmental applications (Loppi et al., 1998, 2019a). Thalli of this species were collected in a remote and reasonably pristine area, far from urban settlements and pollution sources, picked at a height >1.5 m to avoid main soil contamination. The material was enveloped in a plastic net (lichen bag) for the exposure. Three samples were left for the analysis not being exposed (unexposed samples).

The lichen bags were exposed (three bags per site) at the Peggy Guggenheim Collection's building, along a linear transect from the Grand Canal towards the gardens, passing through two halls of the museum, for a total of six sites on the ground floor and one on the rooftop (Fig. 1): the first one, closest to the Grand Canal, tied to the balcony railing (GC), then on the marble ornaments of the external wall of the building (EW); on the windows railings (OH) close to the staircase of entrance by the side of the Grand Canal; in two halls of the museum, the first one with the Picasso's masterpiece "The Studio", in front of the entrance (H1), and the other, on the left facing the Grand Canal, where Boccioni's "Dynamism of a Speeding Horse" and "The Regular" by Marcoussis are displayed (H2). Another site was located on the rooftop terrace, tied to the railing (RO) and the last one on the branches of three *Tilia americana* trees, close to the entrance by the garden side (GA). As far as possible, lichen bags were tied avoiding close contact with metallic parts or furniture. The exposure of the samples lasted 3 months (November 4, 2022–February 6, 2023) and during this period the indoor transplants were sprayed with water to keep thalli hydrated. At the end of the exposure period, samples were retrieved, individually stored in paper bags before being dried until the magnetic and chemical analyses.

2.3. Leaf sampling

Leaves of *P. tobira* were sampled from the available hedges at increasing distances from the Grand Canal at ca. 1 m from the ground: on the terrace with the pier to the Grand Canal (P1, P2, P3), on the opposite side of P3 with respect to the Grand Canal (P4), in the garden, close to the building (P5) and by the side of the street Fondamenta Venier dai Leoni (P10, sampled only in November). In the rooftop, *P. tobira* was sampled at the Grand Canal side (P6, P7), and at the garden side (P8, P9). Two samplings were done: before exposure (4th of November 2022) and at retrieval of lichen samples (6th of February 2023).

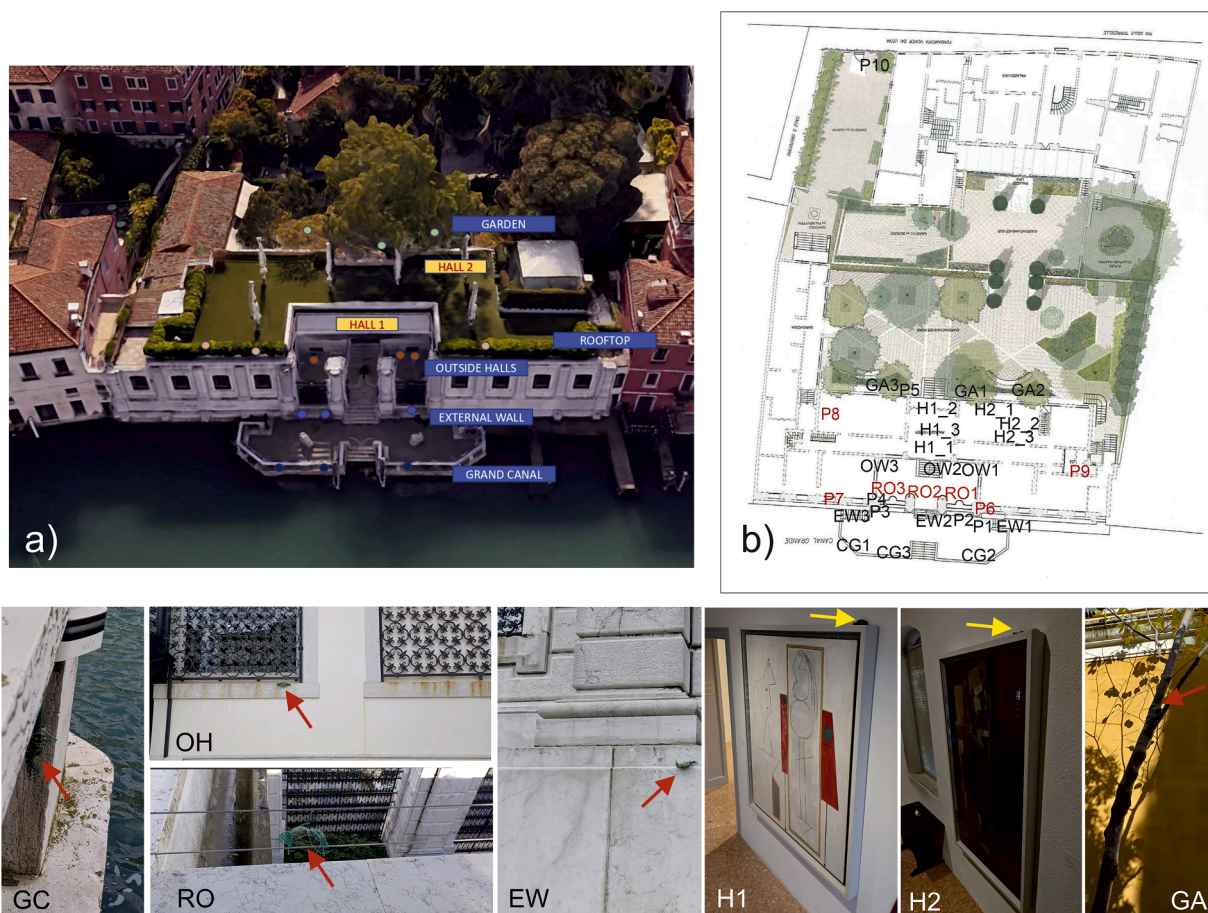


Fig. 1. (a) Google Earth view of the Peggy Guggenheim Collection: the colored dots indicate the lichen bags exposed outdoors (b) lichen and *Pittosporum tobira* sampling sites: the samples at ground level are in black, in red at the rooftop. In the pictures: lichen bags (indicated by red arrows outdoors, yellow indoors) at the sites GC (Grand Canal), OH (Outside Halls), RO (Rooftop), EW (External Wall), H1 (Hall 1 - "The Studio" by Picasso), H2 (Hall 2 - "The Regular" by Marcoussis) and GA (Garden).

2.4. Magnetic analysis

The magnetic properties were measured at the paleomagnetic laboratory of Istituto Nazionale di Geofisica e Vulcanologia in Rome, Italy.

Lichens and leaves were dried with a Bionsec Domus plastic desiccator, for at least 24 h, then placed in 8 cm³ plastic cubes to determine the magnetic susceptibility by mass (χ , m³/kg) with a Agico KLY5 meter. The hysteresis properties, i.e. the coercive force (Bc, T), the saturation remanent magnetization by mass (Mrs, or SIRM, Am²/kg) and the saturation magnetization by mass (Ms, Am²/kg), were investigated on standard gel caps#4 with the magnetic vibrating sample magnetometer Lakeshore 8604 up to a field of 1.0 T in point-by-point discrete sweep mode, at steps of 2.5 mT. Ms and Mrs were determined after subtracting the high field linear trend after saturation, interpolated from 700 to 999 mT. The coercivity of the saturation remanent magnetization (Bcr) was calculated from the logarithmic backfield remagnetization curves up to -1 T, after saturating at 1.0 T. The domain state and magnetic grain size of the samples were compared to theoretical magnetite according to the hysteresis ratios Mrs/Ms and Bcr/Bc in the "Day plot" (Day et al., 1977; Dunlop, 2002a, 2002b). First order reversal curves (FORCs) were measured at steps of 2.5 mT, with 300 ms averaging time and maximum applied field being 1.0 T. FORC diagrams were processed, Variforc smoothed and drawn with the FORCINEL 3.06 Igor Pro routine (Harrison and Feinberg, 2008). FORC diagrams provide information regarding magnetic reversal mechanisms in ferromagnetic minerals (Pike et al., 1999; Roberts et al., 2000) and are used for delineating the distributions of the interaction field (Bu) and coercivity in samples, in order to

distinguish between superparamagnetic (SP), single domain (SD), multidomain (MD) and pseudo-single domain/vortex (PSD/V) behaviors, the latter describing the transitional state between SD and MD particles.

2.5. Chemical analysis

Chemical analyses were performed at the University of Siena, Italy. About 250 mg for each lichen sample was weighted and then acid-digested with 3 mL of HNO₃, 0.2 mL of HF and 0.5 mL of H₂O₂ in a microwave digestion system (Ethos 900, Milestone). Afterwards, the samples were analyzed by ICP-MS (NexION 350x, Perkin Elmer) to quantify the content of Fe, Al, Cu, Ba, Cr, Zn and Sb. ICP-OES (Optima 2000 DV, Perkin Elmer) was used to measure S.

Analytical quality was verified using the certified reference materials IAEA-336 "Lichen" and GBW07604 "Poplar leaves" for Ni and S, not certified in IAEA-336, and was in the range 98–110 %; precision of the analysis was expressed by the relative standard deviation of 3 replicates and was below 3 % for all elements. Three measurements were repeated for each sample and the results were expressed on a dry weight basis.

2.6. Statistical analysis

To disentangle the effect of indoor/outdoor exposure on magnetic and chemical parameters of transplanted lichens, a linear mixed-effects model (LMEM) was fitted for each measured parameter, with exposure as fixed factor and site as random factor. For model validation, the

Levene and Shapiro-Wilk tests were used to check for homoscedasticity and normality, respectively. The significance of the models was checked with type II Anova (analysis of deviance) using the Wald chi-square test. All calculations were run using the R software (R Core Team, 2022).

3. Results

3.1. Magnetic properties

The magnetic susceptibility of *P. tobira* leaves (Table 1) ranged -5.37 – $1.31 \times 10^{-9} \text{ m}^3 \text{ kg}^{-1}$ with a mean value of $-3.06 \pm 0.74 \times 10^{-9} \text{ m}^3 \text{ kg}^{-1}$ in November. After 96 days, magnetic susceptibility ranged -2.73 – $7.01 \times 10^{-9} \text{ m}^3 \text{ kg}^{-1}$ with a mean value of $1.62 \pm 0.90 \times 10^{-9} \text{ m}^3 \text{ kg}^{-1}$. The magnetic susceptibility values of leaves indicated prevailing diamagnetism, suggesting a negligible accumulation of magnetic particles, which discouraged further magnetic analyses, such as hysteresis loops, that were tested on selected samples and confirmed very weak and unreliable magnetic properties, at the sensitivity limits of the VSM. As a mere qualitative test, leaves of *Acanthus mollis* L. were sampled in close proximity to *Pittosporum* P4, and their magnetic susceptibility changed from -0.470 to $12.33 \times 10^{-9} \text{ m}^3 \text{ kg}^{-1}$ during the same period.

The magnetic susceptibility of lichen transplants (Table 1) varied, on average, from $12.90 \pm 4.06 \times 10^{-9} \text{ m}^3 \text{ kg}^{-1}$ indoor to $26.9 \pm 5.30 \times 10^{-9} \text{ m}^3 \text{ kg}^{-1}$ outdoor. One of the lichen bags exposed on the branches of *Tilia americana* in the garden showed a χ approximately one order of magnitude larger than the other two samples of the same site (187.00 vs 19.60 and $30.00 \times 10^{-9} \text{ m}^3 \text{ kg}^{-1}$). For this reason, it was disregarded and considered an outlier (Tukey test), as it was probably contaminated by a point source of pollution, likely a nearby high-power spotlight. The mean χ of unexposed lichen samples was $13.50 \pm 5.40 \times 10^{-9} \text{ m}^3 \text{ kg}^{-1}$. Magnetic susceptibility decreased in the following order from outdoors to indoors (Table 1); χ (EW) > χ (OH) > χ (RO) > χ (GA) > χ (GC) > χ (H2) > χ (H1). The mean values of χ of unexposed and indoor samples differ for $2.22 \times 10^{-9} \text{ m}^3 \text{ kg}^{-1}$, while the difference between the mean outdoor and unexposed samples was about six folds, that is $13.20 \times 10^{-9} \text{ m}^3 \text{ kg}^{-1}$ (Fig. 2).

The hysteresis loops were saturated at relatively low magnetic fields, with Ms, Mrs average values being 1.15 ± 0.46 , 1.88 ± 0.66 and 0.16 ± 0.06 , $0.21 \pm 0.07 \text{ mAm}^2 \text{ kg}^{-1}$, indoors and outdoors, respectively (Table 1). Bc and Bcr spanned 9.1 – 10.7 mT and 22.5 – 34.1 mT , respectively (Table 1), indicating the homogeneous prevalence of low coercivity magnetite-like minerals, under a very limited variation of Bc values. Furtherly, it was calculated the SIRM/ χ ratio, as a proxy of the magnetic grain size of the samples; on average the values were 11.5 ± 5.6 , 12.4 ± 3.9 and $7.6 \pm 1.7 \text{ kA/m}$ for unexposed, indoor and outdoor samples, respectively (Table 1). Overall, statistically significant differences ($p < 0.05$) emerged only between lichen samples exposed outdoors and the others: lichen samples exposed indoors were significantly similar to unexposed samples.

In the Day Plot (Fig. 3), the mean Mrs/Ms and Bcr/Bc ratios were computed and averaged at site level and compared to the exhaust and non-exhaust vehicular emissions from Sagnotti et al. (2009): all sites lie

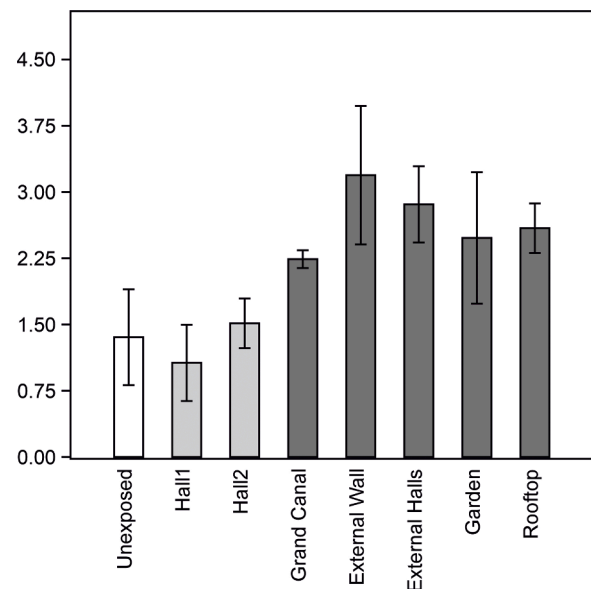


Fig. 2. Mean magnetic susceptibility of lichen transplants, by exposure site ($10^{-8} \text{ m}^3 \text{ kg}^{-1}$, \pm standard deviation): outdoor sites in dark grey, indoor sites in light grey, unexposed samples in white.

on the central/PSD region of the plot, not far from the trend lines that represent the mixtures of SD and MD pure magnetite grains.

The FORC diagrams were computed for selected samples: in Fig. 4, an unexposed sample (a) is compared to the lichen placed over “The Studio” by Picasso (b), and to another tied to the external wall (c). Despite the relatively low magnetic signal and the use of high smoothing factors, especially at the background, it is evident a shift of magnetic properties from the unexposed sample, that mainly shows PSD/Vortex features, to a slight spreading along the Bu axis of the Picasso’s lichen bag, up to the superimposition of viscous properties in the outdoor sample, that can be ascribed to the accumulation of MD or SP particles, as well as to a tri-lobate geometry that is typical for vortex states and particles that may possibly stray into the MD size range (Roberts et al., 2014; Lascu et al., 2018; Sheik et al., 2023). In the outdoor sample, the high coercivity ridge extending beyond magnetite coercivities suggests the presence of metallic Fe (Sheikh et al., 2022)

3.2. Content of PTEs

The concentrations of PTEs are reported in Table 2. Indoors, the prevailing element was zinc (Zn), with an accumulation of 107 % in Hall 2, and 79 % in Hall 1; a minor accumulation was found for nickel (Ni). In the outdoor sites, antimony (Sb) prevailed and stood out over the rooftop where it was more than twice the concentration in unexposed samples, then with a decreasing order, close to Grand Canal (GC), on the wall facing the dock (EW), just outside of the museum (OH) and the

Table 1

Mean \pm standard deviation of mass specific magnetic susceptibility (χ), saturation magnetization (Ms), remanent magnetization (Mrs), coercivity (Bc), coercivity of the remanence (Bcr) and saturation remanent magnetization to magnetic susceptibility ratio (SIRM/ χ) of the lichen bags and unexposed samples. The asterisk indicates that the Mean \pm standard deviation is computed disregarding an outlier.

| | χ ($10^{-8} \text{ m}^3 \text{ kg}^{-1}$) | Ms ($\text{mAm}^2 \text{ kg}^{-1}$) | Mrs ($\text{mAm}^2 \text{ kg}^{-1}$) | Bc (mT) | Bcr (mT) | SIRM/ χ (kAm^{-1}) |
|---------------|--------------------------------------------------|---------------------------------------|----------------------------------------|------------------|------------------|------------------------------------|
| Unexposed | 1.35 ± 0.54 | 0.93 ± 0.02 | 0.14 ± 0.01 | 10.40 ± 0.17 | 27.52 ± 1.97 | 11.54 ± 5.61 |
| Hall 1 | 1.07 ± 0.43 | 1.10 ± 0.62 | 0.16 ± 0.05 | 10.60 ± 0.10 | 27.81 ± 5.57 | 14.20 ± 4.32 |
| Hall 2 | 1.51 ± 0.28 | 1.19 ± 0.35 | 0.16 ± 0.01 | 10.20 ± 0.52 | 31.16 ± 1.37 | 10.69 ± 3.06 |
| Outside Halls | 2.86 ± 0.43 | 2.15 ± 0.30 | 0.24 ± 0.04 | 9.84 ± 0.31 | 30.79 ± 1.80 | 8.43 ± 0.46 |
| External wall | 3.19 ± 0.71 | 2.25 ± 0.80 | 0.23 ± 0.09 | 9.33 ± 0.40 | 32.80 ± 1.19 | 7.01 ± 1.77 |
| Grand Canal | 2.24 ± 0.10 | 1.40 ± 0.20 | 0.16 ± 0.01 | 9.89 ± 0.54 | 31.27 ± 1.60 | 7.33 ± 0.53 |
| Garden* | 2.48 ± 0.74 | 1.75 ± 1.12 | 0.21 ± 0.13 | 9.80 ± 0.21 | 30.56 ± 1.38 | 7.93 ± 3.21 |
| Rooftop | 2.59 ± 0.28 | 1.78 ± 0.87 | 0.20 ± 0.09 | 9.82 ± 0.15 | 32.39 ± 2.14 | 7.60 ± 2.89 |

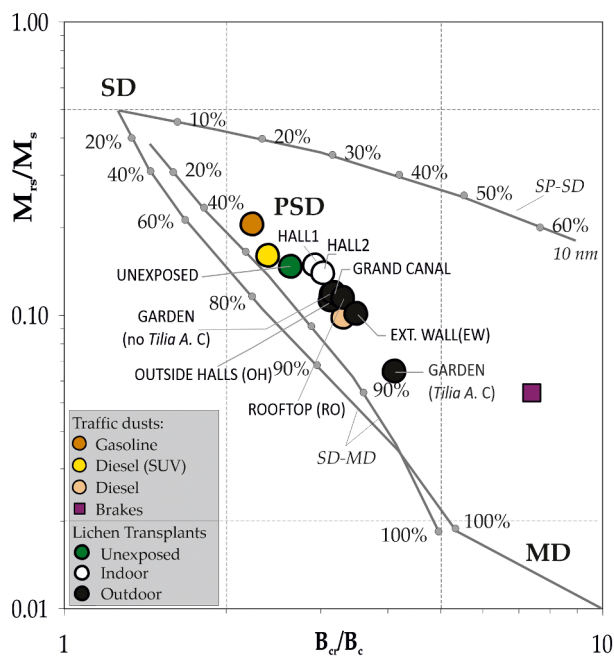


Fig. 3. Bilogarithmic “Day plot” (Day et al., 1977) of the site averaged hysteresis ratios for lichen transplants (black circles for outdoor sites, white circles for indoor sites, green circle for unexposed samples), reported together with the average points for different kinds of fuel exhaust (orange, yellow and pink circles) and brake dust emissions (purple square) calculated from Sagnotti et al. (2009). The SD (single domain), PSD (pseudo-single domain) and MD (multi-domain) fields and the theoretical mixing trends for SD-MD and SP-SD pure magnetite particles (SP, superparamagnetic) are from Dunlop (2002a, 2002b).

garden (GA).

The net sulphur accumulation stood out close to the Grand Canal (+56 %) but was very low or absent at the other sites. Sites outdoors, close to the museum (EW, OH, RO sites), showed the accumulation of Zn, maximum in RO (142 %), followed by indoor sites (106 % H2, 79 % H1); the accumulation of Zn decreased as the distance from the museum to the Grand Canal increased. The amount of copper (Cu) was relevant in two outdoor sites (EW, RO). The content of Aluminum (Al) varied remarkably just at two sites, GA and RO with an accumulation of 37 % and 38 %, respectively. Iron, Barium and Chromium did not show any particular accumulation (maximum 18 % for Fe at EW).

Overall, as opposed to magnetic data, statistically significant

differences did not emerge between lichen samples unexposed, or exposed indoors and outdoors.

4. Discussion

Combined magnetic and chemical analysis of lichen transplants and *Pittosporum* leaves provided a complex and detailed overview of the airborne PTEs present indoors and outdoors of the Peggy Guggenheim Collection, by both qualitative and quantitative profiles.

Magnetic susceptibility is among the most used parameters in bio-magnetic monitoring of airborne PM: it is cost-effective and very sensitive even to very low concentrations of magnetic minerals. χ values can show the accumulation of ferrimagnetic fractions of PM even at barely detectable levels. Despite this, the magnetic susceptibility values of *P. tobira* leaves were so low to consider their bioaccumulation of magnetic particles substantially negligible. In fact, the whole dataset but one sample, in November 2022, was diamagnetic, with a very weak increase in February 2023, that was so limited to reach $7.09 \times 10^{-9} \text{ m}^3 \text{ kg}^{-1}$ as the maximum value. Winkler et al. (2022) discussed the role of tree and shrub leaves for providing preventive conservation services. The concentration dependent magnetic parameters of *Platanus orientalis* leaves doubled after three months of exposure in Rome, in Lungotevere Farnesina, despite Muhammad et al. (2019) classified the species in the group characterized by the lowest bioaccumulation of magnetic particles. In this study, after three months, *Pittosporum* leaves did not substantially change their magnetic susceptibility values, highlighting negligible concentration of airborne magnetic particles or their unsuitability for their immobilization. Conversely, Lorenzini et al. (2006) showed that *P. tobira* is a suitable passive biodeposimeter, useful to assess levels and distribution patterns of inorganic solid pollutants in urban areas. However, during the investigated period, for 20 days out of 90 the daily PM_{10} concentration levels exceeded the EU limit of $50 \mu\text{g}/\text{m}^3$, as recorded by automated monitoring stations of air quality in Venice downtown (<https://www.arpa.veneto.it/dati-ambientali/dati-storici/aria/qualita-dellaria-storico-dati-validati>). For 6 consecutive days right before sampling the leaves in February, PM_{10} concentration exceeded the limit, reaching values as high as $107 \mu\text{g}/\text{m}^3$ along with an event of persistent high pressure that caused abnormally low tide. Thus, it is possible to conclude that, at least in this aquatic lagoon context, *Pittosporum tobira* leaves did not behave as efficient bioaccumulator.

Moreover, the leaves of *Achantus mollis* that were sampled close to *P. tobira* leaves (P4) on the opposite side of the plant, with respect to the Grand Canal, showed that χ value increased by $12.70 \times 10^{-9} \text{ m}^3 \text{ kg}^{-1}$, with respect to $4.05 \times 10^{-9} \text{ m}^3 \text{ kg}^{-1}$ of P4, thus confirming the limited bioaccumulation of this species.

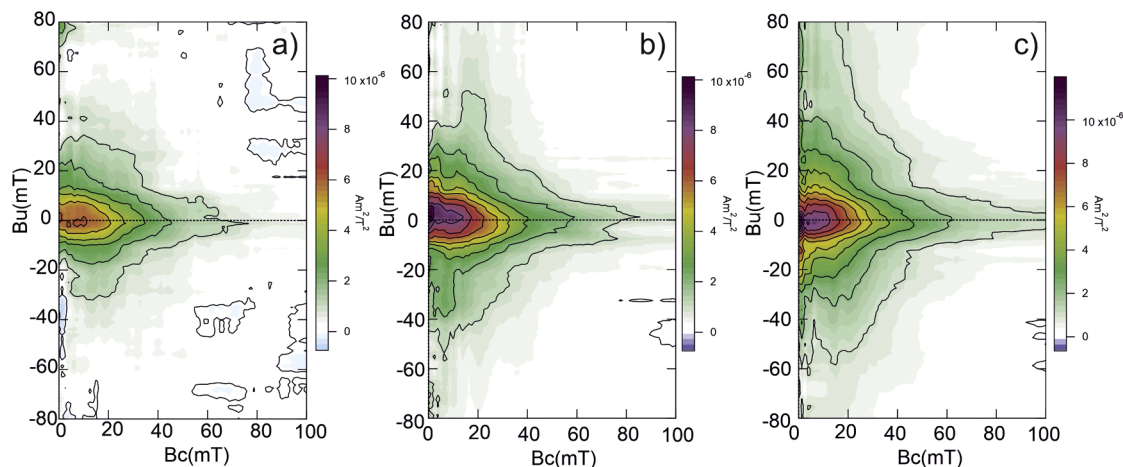


Fig. 4. FORC diagrams, for a selected unexposed lichen bag (a), for the bag exposed over “The Studio” by Picasso (b) and at the external wall (c); averaging time was 300 ms and variforc smoothed up to 12 at the background.

Table 2

Mean element concentration ($\mu\text{g/g dw}$, \pm standard deviation) in lichen samples. The asterisk indicates that the Mean \pm standard deviation is computed disregarding an outlier.

| | S | Fe | Al | Cu | Zn | Ba | Cr | Sb | Ni | V |
|---------------|----------------|---------------|---------------|----------------|-----------------|----------------|-----------------|-------------------|-------------------|-------------------|
| Unexposed | 900 \pm 96 | 637 \pm 126 | 404 \pm 79 | 6.9 \pm 0.7 | 21.8 \pm 5.1 | 14.4 \pm 1.9 | 1.8 \pm 0.2 | 0.097 \pm 0.015 | 2.942 \pm 0.617 | 1.929 \pm 0.351 |
| Hall 1 | 744 \pm 26 | 554 \pm 128 | 433 \pm 60 | 6.9 \pm 0.6 | 39.0 \pm 0.8 | 13.3 \pm 0.6 | 1.7 \pm 0.6 | 0.106 \pm 0.028 | 4.135 \pm 1.322 | 1.682 \pm 0.407 |
| Hall 2 | 963 \pm 148 | 652 \pm 90 | 401 \pm 67 | 7.3 \pm 0.5 | 45.0 \pm 14.2 | 15.0 \pm 0.3 | 1.8 \pm 0.1 | 0.108 \pm 0.015 | 3.536 \pm 0.647 | 1.938 \pm 0.292 |
| Outside Halls | 898 \pm 54 | 749 \pm 142 | 470 \pm 135 | 7.5 \pm 0.2 | 35.2 \pm 7.6 | 19.0 \pm 3.8 | 2.0 \pm 0.4 | 0.194 \pm 0.040 | 2.159 \pm 0.496 | 2.159 \pm 0.554 |
| External wall | 843 \pm 235 | 621 \pm 198 | 367 \pm 154 | 11.9 \pm 2.0 | 34.8 \pm 8.4 | 14.0 \pm 1.8 | 1.95 \pm 0.36 | 0.220 \pm 0.011 | 1.667 \pm 0.454 | 1.759 \pm 0.516 |
| Grand Canal | 1404 \pm 269 | 460 \pm 29 | 259 \pm 69 | 7.9 \pm 0.1 | 21.0 \pm 0.7 | 14.3 \pm 1.3 | 1.75 \pm 0.34 | 0.244 \pm 0.080 | 3.323 \pm 3.523 | 1.516 \pm 0.172 |
| Garden* | 1002 \pm 189 | 582 \pm 53 | 554 \pm 232 | 7.0 \pm 0.0 | 19.2 \pm 1.8 | 13.5 \pm 1.2 | 1.7 \pm 0.4 | 0.159 \pm 0.005 | 1.639 \pm 0.592 | 1.757 \pm 0.135 |
| Rooftop | 980 \pm 121 | 538 \pm 56 | 557 \pm 49 | 11.4 \pm 1.8 | 52.8 \pm 2.2 | 14.0 \pm 0.1 | 1.91 \pm 0.29 | 0.259 \pm 0.028 | 2.074 \pm 0.209 | 1.548 \pm 0.258 |

As far as lichen transplants are concerned, χ values resulted highly correlated with those of Ms and Mrs, the concentration dependent magnetic parameters determined from hysteresis loops. Considering the higher sensitivity and representativeness of the magnetic susceptibility measurements, carried out on standard 8 cc cubes instead of 0.2 mL gel caps, hysteresis properties were mostly interpreted in the light of magnetic mineralogy analyses, leaving the quantitative aspects to χ . By the comparison of χ values of lichen transplants, a significant statistical difference ($p < 0.05$) was found between the indoor and outdoor sites, with outdoor values, on average, twice those indoors ($2.67 \times 10^{-8} \text{ m}^3 \text{ kg}^{-1}$ vs $1.29 \times 10^{-8} \text{ m}^3 \text{ kg}^{-1}$, respectively), being $1.35 \times 10^{-8} \text{ m}^3 \text{ kg}^{-1}$ the mean of the unexposed samples. Thus, three months of exposure were enough to distinguish two main clusters of samples according to χ values: a statistical difference was found between unexposed samples and outdoor samples but not between unexposed and indoor samples. The same conclusion was confirmed by Ms and Mrs values, the concentration dependent magnetic parameters obtained from hysteresis loops.

For what concerns the prevailing magnetic grain-size/domain state, in the "Day plot" all samples fell in the central region of the diagram, where are usually located natural and exhaust vehicular magnetic components, as opposed to non-exhaust emissions that prevail in vehicular traffic urban context, which are placed in the lower-right side of the plot (Sagnotti et al., 2009; Winkler et al., 2020, 2021; Gonet et al., 2021a, b). In detail, the unexposed samples fell in the upper left PSD region of the plot, with the indoor and outdoor sites progressively shifting towards slightly higher proportions of coarser MD particles. The outlier transplant tied to a *Tilia* a. in the garden confirms to be anomalous also for its coarser magnetic grain size.

As a reference, the critical magnetic grain-size transitions, theoretically determined for equidimensional magnetite, are about 0.03 μm for SP to SD, 0.08 μm for SD to PSD, and 17 μm for PSD to true MD (Butler et al., 1975), the gradual transition from SD to true MD depending on the spontaneous magnetization, shape and the state of internal stress of a particle (Roberts et al., 2017).

This result is also consistent with the features of the FORC diagrams, that showed a progressive increase of vertically spread magnetic components in the indoor and, especially, the outdoor samples, within predominant vortex/PSD general aspects. In Sheikh et al. (2022), the apparent MD signal observed in brake pad residues was attributed to a combination of high-coercivity ridge and a low-coercivity vertically spread signal, which Lappe et al. (2013) considered consistent with the presence of metallic particles in vortex states. It is supposed that the bioaccumulated particles are in the grain-size range from the upper end of the vortex state to MD behavior, with a peak at the origin that can be attributed to an ultrafine SP component, with the high coercivity ridge possibly related to the presence of metallic Fe.

SIRM/ χ values confirm this trend too: the mean values of the outdoor samples were lower than those indoor and unexposed, that are very

similar, highlighting the relative increased income of coarser magnetic particles.

On the whole dataset, χ values were not dependent on the concentration of Fe (Fig. 5), indicating that the most Fe is not directly linked to magnetic minerals, that are the main carriers of magnetic susceptibility. Thus, following the different groups of samples as emerged by the statistical analysis of magnetic susceptibility values, the linear correlation between Fe and χ was tested splitting the dataset into the unexposed + indoor and outdoor samples. In this way, two different and significant linear trends were found (Fig. 5), confirming the different bioaccumulation of magnetic particles outdoors, with respect to the indoor and unexposed samples. It is supposed that the presence of Fe is mainly linked to paramagnetic/weak bioaccumulation conditions in the indoor and unexposed samples, with a moderate supply of further paramagnetic and ferrimagnetic components recorded outdoors.

According to the Ms values, that is a grain size independent magnetic parameter, and after the assumption that the magnetic mineralogy is compatible with magnetite-like minerals, whose mass Ms value is 90 Am^2/kg (Dunlop and Ozdemir, 1997), it is possible to calculate the weight percentage (wt%) of magnetite in the samples. Averaged at site level, wt% (EW) > wt% (OH) > wt% (RO) > wt% (GA) > wt% (GC) > wt% (H2) > wt% (H1) > wt% (UN) (Table 3).

As a qualitative test, it was evaluated the percentage ratio % ($\text{Fe}_{\text{magnetite}}/\text{Fe}_{\text{tot}}$), that is indicative of the percentage fraction of magnetite's iron within the total concentration of Fe. $\text{Fe}_{\text{magnetite}}$ was calculated according to the weight percentage of iron in magnetite, that is 72%. Under this approach, it was possible to estimate that all the lichen transplants accumulated magnetite, and its associated iron in outdoor samples was about 4 times higher than indoors (Table 3).

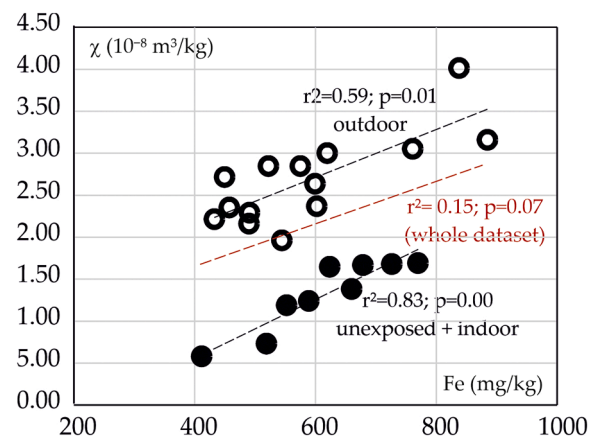


Fig. 5. Relationship between χ and Fe in the whole dataset (red dashed line), and splitting outdoor (white) and indoor+unexposed (black) samples.

Table 3

Weight percentage content of magnetite and elemental Fe, % ratio of the presence of magnetite within the total Fe content and its differential with respect to unexposed samples, indicated as $\Delta\%(\text{Fe}_{\text{magnetite}}/\text{Fe}_{\text{tot}})$. The asterisk indicates that the Mean \pm standard deviation is computed disregarding an outlier.

| | wt% (magnetite) | wt% (Fe) | %($\text{Fe}_{\text{magnetite}}/\text{Fe}_{\text{tot}}$) | $\Delta\%(\text{Fe}_{\text{magnetite}}/\text{Fe}_{\text{tot}})$ |
|------------------|-----------------------|-----------------------|------------------------------------------------------------|-----------------------------------------------------------------|
| Unexposed | 1.04×10^{-3} | 6.37×10^{-2} | 1.17 | |
| Hall 1 | 1.22×10^{-3} | 5.54×10^{-2} | 1.59 | +0.42 |
| Hall 2 | 1.32×10^{-3} | 6.52×10^{-2} | 1.46 | +0.29 |
| Outside Halls | 2.39×10^{-3} | 7.49×10^{-2} | 2.29 | +1.12 |
| External wall | 2.50×10^{-3} | 6.21×10^{-2} | 2.90 | +1.73 |
| Grand Canal | 1.56×10^{-3} | 4.60×10^{-2} | 2.44 | +1.27 |
| Garden* | 1.95×10^{-3} | 5.82×10^{-2} | 2.41 | +1.24 |
| Rooftop | 1.98×10^{-3} | 5.38×10^{-2} | 2.66 | +1.49 |

Overall, indoor lichens showed a modest environmental impact: from a magnetic point of view, after three months of exposure, the indoor bioaccumulation of metallic particles was negligible, and barely detectable from a grain-size point of view. Conversely, a moderate bioaccumulation was measured outdoors, corresponding to 2.4 as the maximum ratio between the magnetic susceptibility of outdoor sites (EW) and that of the unexposed samples, which is 17 times lower with respect to the study in Villa Farnesina, where the lichens tied to *Platanus* trees along the Lungotevere highlighted χ values 39.3 times higher than unexposed samples (Winkler et al., 2022).

It should also be noted that the average χ values of the unexposed samples in Villa Farnesina was $0.6 \times 10^{-8} \text{m}^3 \text{kg}^{-1}$ while in the present study it was $1.3 \times 10^{-8} \text{m}^3 \text{kg}^{-1}$, thus implying a different baseline and sensitivity in the determination of the relative bioaccumulations. Also the FORC diagrams outlined that relevant magnetic components were already carried by the unexposed samples (Fig. 4a).

Outdoors, the Day Plot, the FORC diagrams and the SIRM/ χ values highlighted the presence of coarser particles, with respect to the indoor and unexposed samples. Masiol et al. (2014) reported that in the aerosol of a semi-rural coastal site near Venice the anthropogenic elements Fe and Zn in the coarse mode ($>4 \mu\text{m}$) were well correlated and probably linked to tire and brake wear emissions. S, K, Mn, Cu, Fe and Zn were strongly inter-correlated in the submicrometric ($<1 \mu\text{m}$) range and Mn, Cu, Zn, Ni in the intermediate mode (1–4 μm), their relationships highlighting the presence of several sources (combustions, secondary aerosol, road traffic). In the intermediate mode, associations having geochemical significance exist between marine (Na, Cl and Mg) and crustal (Si, Mg, Ca, Al, Ti and K) elements. Strong winds favor the formation of sea-spray and the increase of Si in the coarse mode due to the resuspension of sand fine particles.

In Prodi et al. (2009), who reviewed the aerosol fine fraction in the Venice Lagoon, the marine aerosol contribution to PM_{10} and $\text{PM}_{2.5}$ fractions, calculated using Na^+ as a tracer of sea-salts, was estimated to be low, in the range 1–6 %. They concluded that Mn and Fe can be partially associated with vehicular traffic, while the high Cr concentration with respect to urban areas is due to industrial activity (e.g. waste incinerator). They also showed that Venice suffers from African dust events, like other Italian cities, that involve much higher concentrations of Si, S, Ca, Ti, P. However, Sagnotti et al. (2006) concluded that the magnetic properties of PM_{10} are not influenced by the presence of high concentration of North African dust, whose magnetic susceptibility is negligible, as well as the marine aerosols, since sea salt is almost diamagnetic. Conversely to that, Larrasoana et al. (2021) concluded that during intense periods of north African dust transport in southwestern

Europe part of the PSD/vortex and MD magnetite grains load is aeolian in origin.

For what concerns shipping emissions, they generally derive from the combustion of so-called “bunker fuel”. Most studies have focused on NO_x , SO_2 , CO and CO_2 as they constitute the majority of ship-derived emissions. Fe-bearing particles occur in the $\text{PM}_{2.5}$ fraction in concentrations up to $10 \mu\text{g}/\text{m}^3$, usually accompanied by other metals, including V, Ni, Zn, Ca, Na, P, where the Fe-rich particles group, constitutes 3, 4 % of all PM mass, with smaller portions of Si, S and Ca. Shipping-derived Fe-bearing particles occur usually in the fraction $<100 \text{nm}$ (Popovicheva et al., 2012; Gonet and Maher, 2019).

The magnetic fingerprint of airborne particulate matter was significantly detectable only in the lichen samples transplanted outdoors, where the moderate increase of the concentration dependent magnetic parameters is related to the bioaccumulation of relatively coarser particles containing magnetite as the main magnetic mineral, in connection with long range industrial and transportation/traffic related activities that are supposed to be largely diffused and far from the study site. In fact, the homogeneous distribution of the outdoor magnetic parameters is well distinct from the exponential decrease of magnetic susceptibility values that is usually observed within few tens of meters from the emission source of magnetic particles (Szönyi et al., 2008, Winkler et al., 2022). It cannot be excluded that a part of the bioaccumulated dusts is of natural aeolian origin. On the other hand, magnetic measurements will discriminate non-exhausts from other magnetic emissions, but fuel exhausts and fine natural magnetic components are somehow difficult to be unmixed (Winkler et al., 2022; Larrasoana et al., 2021). Irrespective of this indeterminacy, for what concerns the main aim of this study, it can be concluded that the indoor bioaccumulation of airborne magnetic particles was negligible.

Biomonitoring such as lichens give a biological response in terms of effect (bioaccumulation in this case) of air pollutants, while physico-chemical devices measure the actual atmospheric concentrations of pollutants. It is known that lichen transplants can profitably be used also indoors, since their vitality is preserved and their response is similar to outdoor samples (Paoli et al. 2019).

To explain the fact that instrumental monitoring showed a remarkable PM_{10} concentration during the exposure period, while lichens exposed outdoors did not show high levels of PTEs, it may be argued that although massively suspended in the air, the deposition rate of PM was low and hence the ability of lichens to intercept it was reduced, as it is well known that biomonitors provide an accurate estimate of bulk element deposition, but not atmospheric concentration (Loppi and Paoli, 2015; Loppi et al., 2019b; Vannini et al., 2019). On the other hand, another possibility is that high humidity levels, as very commonly experienced in the lagoon of Venice, can lead to leaching, where previously accumulated trace elements within lichen pseudo-tissues can be washed out, resulting in a reduced bioaccumulation, as elements are lost from the lichens. However, the influence of humidity on bioaccumulation is complex and may depend on the interplay of various factors, including local atmospheric composition, wind patterns, and the physiological characteristics of the lichens themselves.

Lichen samples exposed outdoors, although not statistically significant, experienced relatively higher values of Sb, which is usually taken as an indicator of non-exhaust (brake wearing) vehicle pollution. However, in the peculiar environment of Venice, vehicle traffic is extremely limited, and cannot be considered a pollution source worthy of consideration. In fact, outdoor χ and Sb were not at all correlated ($R^2=0.00$, $p = 0.99$), thus confirming that Sb is not linked to magnetic emissions from brakes, as opposed to what happens in vehicular traffic contexts (Winkler et al., 2021, 2020). Nevertheless, high Sb levels are common in the Venice lagoon owing to the massive use of this element in traditional artistic venetian glasswork (Formenton et al., 2021). When added to the glass, beside producing a range of colors, especially yellow, the presence of antimony can also affect the refractive index and opacity of the glass, contributing to its aesthetic and artistic qualities. The

relatively higher values of Zn measured indoors and at some sites outdoors may be related with the use of zinc oxide which is employed as desiccant in applications related to dehumidification due to its ability to absorb moisture. Zinc oxide's moisture-absorbing properties make it useful in various scenarios where controlling humidity is important, as it is typical in Venice.

5. Conclusions

In this study, a magnetic and chemical biomonitoring approach was tested for assessing the diffusion of metallic PM from the Grand Canal to the halls of the Peggy Guggenheim Collection in Venice, Italy. Lichen bags were exposed outside on both sides of the museum, at increasing distances from the Grand Canal. Indoors, they were located inside two halls, hosting masterpieces by Picasso, Marcoussis and Boccioni. Leaves of *Pittosporum tobira* were sampled at the beginning and at the end of the lichen exposure period, in order to evaluate their suitability for providing biomonitoring and ecosystemic services.

Lichen transplants were effective for outlining that the bioaccumulation of metallic particles was negligible indoors and moderate outdoors. Indoors, the concentration dependent magnetic parameters were statistically similar to those of unexposed samples. Outdoors, the bioaccumulation of metallic particles was ascribed to magnetic fractions in coarser vortex to multidomain range, with respect to the vortex components already present in the unexposed samples.

Pittosporum tobira leaves mostly showed diamagnetic properties, being unsuited for both magnetic biomonitoring and preventive conservation purposes.

The concentration dependent magnetic parameters were mostly homogenous outdoors, with a limited decrease of the magnetic susceptibility values with the distance from the Grand Canal. It is hypothesized that their main sources are diffused or distant from the study site, as a mixture of anthropogenic and natural far driven dusts.

Magnetic biomonitoring demonstrated to be a very sensitive methodology for outlining the impact of metallic emissions, assessed in terms of the composition, concentration and grain-size distribution of iron oxides. Magnetic analyses were so sensitive to detect minimal variations in the concentration levels of Fe, that can be associated with ferrimagnetism and discriminate against different sources of PM, especially when chemical analysis did not reveal any statistically significant difference between lichen bags exposed outdoors and indoors.

CRedit authorship contribution statement

Lisa Grifoni: Methodology, Validation, Formal analysis, Investigation, Writing – original draft. **Aldo Winkler:** Conceptualization, Methodology, Validation, Formal analysis, Investigation, Writing – original draft, Supervision, Funding acquisition. **Luigi Antonello Di Lella:** Formal analysis. **Luciano Pensabene Buemi:** Investigation, Supervision, Methodology. **Antonio Sgamellotti:** Conceptualization, Investigation, Supervision, Methodology. **Lilla Spagnuolo:** Formal analysis. **Stefano Loppi:** Conceptualization, Methodology, Validation, Formal analysis, Investigation, Writing – original draft, Supervision.

Declaration of Competing Interest

The authors declare that they have no known competing financial interests or personal relationships that could have appeared to influence the work reported in this paper.

Data availability

Data will be made available on request.

Acknowledgments

This research was funded by INGV Project “Pianeta Dinamico” (Ministry of University and Research), research line 2023-2025 “CHIOMA”, Cultural Heritage Investigations and Observations: a Multidisciplinary Approach.

The Lakeshore 8604 VSM was funded by the Ministry of University and Research, project PON GRINT, code PIR01_00013.

The authors would like to thank Siro De Boni for his fundamental help during the sampling and exposure operations. The authors would like to thank the referees and the editors for their great care.

The article is dedicated to the loving memory of Laura Sgamellotti.

References

- Almeida, S.M., Canha, N., Silva, A., Freitas, M.D., Pegas, P., Alves, C., Evtyugina, M., Pio, C.A., 2011. Children exposure to atmospheric particles in indoor of Lisbon primary schools. *Atmos. Environ.* 45, 7594–7599.
- Butler, R.F., Banerjee, S.K., 1975. Theoretical single-domain grain size range in magnetite and titanomagnetite. *J. Geophys. Res.* 80, 4049–4058.
- Canha, N., Almeida, S.M., Freitas, M.C., Wolterbeek, H.T., 2014. Indoor and outdoor biomonitoring using lichens at urban and rural primary schools. *J. Toxicol. Environ. Health Part A* 77, 900–915. <https://doi.org/10.1080/15287394.2014.911130>, 14–16.
- Chaparro, M.A.E., 2021. Airborne particle accumulation and loss in pollution-tolerant lichens and its magnetic quantification. *Environ. Pollut.*, 117807 <https://doi.org/10.1016/j.envpol.2021.117807>.
- Comite, V., Pozo-Antonio, J.S., Cardell, C., Rivas, T., 2019. Metals distributions within black crusts sampled on the facade of an historical monument: The case study of the Cathedral of Monza (Milan, Italy). *IMEKO TC4 International. In: Conference on Metrology for Archaeology and Cultural Heritage, MetroArcheo: 4 through 6 December. International Measurement Federation Secretariat (IMEKO)*, pp. 73–78.
- Day, R., Fuller, M., Schmidt, V.A., 1977. Hysteresis properties of titanomagnetites: grain-size and compositional dependence. *Phys. Earth Planet. Inter.* 13, 260–267. [https://doi.org/10.1016/0031-9201\(77\)90108-X](https://doi.org/10.1016/0031-9201(77)90108-X).
- Dunlop, D.J., 2002a. Theory and application of the day plot (MRS/MS versus HCR/HC) 1. Theoretical curves and tests using titanomagnetite data. *J. Geophys. Res.* 107. <https://doi.org/10.1029/2001JB000487>.
- Dunlop, D.J., 2002b. Theory and application of the day plot (MRS/MS versus HCR/HC) 2. Application to data for rocks, sediments, and soils. *J. Geophys. Res.* 107. <https://doi.org/10.1029/2001JB000486>.
- Dunlop, D.J., Ozdemir, O., 1997. *Rock Magnetism: Fundamentals and Frontiers*. Cambridge University Press, Cambridge.
- Formenton, G., Gregio, M., Gallo, G., Liguori, F., Peruzzo, M., Innocente, E., Lava, R., Masiol, M., 2021. PM10-bound arsenic emissions from the artistic glass industry in Murano (Venice, Italy) before and after the enforcement of REACH authorisation. *J. Hazard. Mater.* 406, 124294 <https://doi.org/10.1016/j.jhazmat.2020.124294>. Article.
- Georgeaud, V.M., Rochette, P., Ambrosi, J.P., Vandamme, D., Williamson, D., 1997. Relationship between heavy metals and magnetic properties in a large polluted catchment: the etang de berre (south of France). *Phys.Chem. Earth* 22 (1–2), 211–214. [https://doi.org/10.1016/S0079-1946\(97\)00105-5](https://doi.org/10.1016/S0079-1946(97)00105-5).
- Gonet, T., Maher, B.A., 2019. Airborne, vehicle-derived Fe-bearing nanoparticles in the urban environment—a review. *Environ. Sci. Technol.* 53, 9970–9991.
- Gonet, T., Maher, B.A., Kukutschová, J., 2021a. Source apportionment of magnetite particles in roadside airborne particulate matter. *Sci. Total Environ.* 752, 141828 <https://doi.org/10.1016/j.scitotenv.2020.141828>.
- Gonet, T., Maher, B.A., Nyiró-Kósa, I., Pósfai, M., Vaculík, M., Kukutschová, J., 2021b. Size-resolved, quantitative evaluation of the magnetic mineralogy of airborne brake-wear particulate emissions. *Environ. Pollut.* 288, 117808 <https://doi.org/10.1016/j.envpol.2021.117808>. Article.
- Harrison, R.J., Feinberg, J.M., 2008. FORCinel: An improved algorithm for calculating first-order reversal curve distributions using locally weighted regression smoothing. *Geochem. Geophys. Geosyst.* 9 (5), 1987. <https://doi.org/10.1029/2008GC001987>.
- Hofman, J., Maher, B.A., Muxworthy, A.R., Wuyts, K., Castanheiro, A., Samson, R., 2017. Biomagnetic monitoring of atmospheric pollution: A review of magnetic signatures from biological sensors. *Environ. Sci. Technol.* 51, 6648–6664. <https://doi.org/10.1021/acs.est.7b00832>.
- Hunt, A., Jones, J., Oldfield, F., 1984. Magnetic measurements and heavy metals in atmospheric particulates of anthropogenic origin. *Sci. Total Environ.* 33, 129–139.
- Lappe, S.C.L.L., Feinberg, J.M., Muxworthy, A., Harrison, R.J., 2013. Comparison and calibration of nonheating paleointensity methods: a case study using dusty olivine. *Geochem. Geophys. Geosyst.* 14 (7), 2143–2158. <https://doi.org/10.1002/ggge.20141>.
- Larrasoana, J.C., Pey, J., Zhao, X., Heslop, D., Mochales, T., Mata, P., Beamud, E., Reyes, J., Cerro, J.C., Perez, N., Castillo, S., 2021. Environmental magnetic fingerprinting of anthropogenic and natural atmospheric deposition over southwestern Europe. *Atmos. Environ.* 261, 118568 <https://doi.org/10.1016/j.atmosenv.2021.118568>. Article.
- Lascu, I., Einsle, J.F., Ball, M.R., Harrison, R.J., 2018. The vortex state in geologic materials: a micromagnetic perspective. *J. Geophys. Res. Solid Earth* 123, 7285–7304. <https://doi.org/10.1029/2018JB015909>.

- Loppi, S., Pacioni, G., Olivieri, N., di Giacomo, F., 1998. Accumulation of trace metals in the lichen *Evernia prunastri* transplanted at biomonitoring sites in Central Italy. *Bryologist* 101 (3), 451–454. <https://doi.org/10.2307/3244187>.
- Loppi, S., Paoli, L., 2015. Comparison of the trace element content in transplants of the lichen *Evernia prunastri* and in bulk atmospheric deposition: a case study from a low polluted environment (C Italy). *Biologia* 70, 460–466 (Bratisl).
- Loppi, S., Ravera, S., Paoli, L., 2019a. Coping with uncertainty in the assessment of atmospheric pollution with lichen transplants. *Environ. Forensics*. <https://doi.org/10.1080/15275922.2019.1627615>.
- Loppi, S., Corsini, A., Paoli, L., 2019b. Estimating environmental contamination and element deposition at a urban area of Central Italy. *Urban Sci.* 3, 76. <https://doi.org/10.3390/urbansci3030076>.
- Lorenzini, G., Grassi, C., Nali, C., Petiti, A., Loppi, S., Tognotti, L., 2006. Leaves of *Pittosporum tobira* as indicators of airborne trace element and PM10 distribution: three case studies from Italy. *Atmos. Environ.* 40 (22), 4025–4036. <https://doi.org/10.1016/j.atmosenv.2006.03.032>.
- Maher, B.A., Moore, C., Matzka, J., 2008. Spatial variation in vehicle-derived metal pollution identified by magnetic and elemental analysis of roadside tree leaves. *Atmos. Environ.* 42, 364–373.
- Masiol, M., Squizzato, S., Ceccato, D., Pavoni, B., 2014. The size distribution of chemical elements of atmospheric aerosol at a semi-rural coastal site in Venice (Italy). The role of atmospheric circulation. *Chemosphere* 119, 400–406. <https://doi.org/10.1016/j.chemosphere.2014.06.086>. PMID: 25063963.
- Muhammad, S., Wuys, K., Samson, R., 2019. Atmospheric net particle accumulation on 96 plant species with contrasting morphological and anatomical leaf characteristics in a common garden experiment. *Atmos. Environ.* 202, 328–344. <https://doi.org/10.1016/j.atmosenv.2019.01.015>.
- Paoli, L., Fačková, Z., Guttová, A., Maccelli, C., Kresáňová, K., Loppi, S., 2019. *Evernia* goes to school: bioaccumulation of heavy metals and photosynthetic performance in lichen transplants exposed indoors and outdoors in public and private environments. *Plants* 8, 125. <https://doi.org/10.3390/plants8050125>.
- Pike, C.R., Roberts, A.P., Verosub, K.L., 1999. Characterizing interactions in fine magnetic particle systems using first order reversal curves. *J. Appl. Phys.* 85, 6660–6667.
- Popovicheva, O., Kireeva, E., Persiantseva, N., Timofeev, M., Bladt, H., Ivleva, N.P., Niessner, R., Moldanova, J., 2012. Microscopic characterization of individual particles from multicomponent ship exhaust. *J. Environ. Monit.* 14, 3101–3110.
- Prodi, F., Belosi, F., Contini, D., Santachiara, G., Di Matteo, L., Gambaro, A., Donato, A., Cesari, D., 2009. Aerosol fine fraction in the Venice Lagoon: particle composition and sources. *Atmos. Res.* 92, 141–150.
- Protano, C., Owczarek, M., Antonucci, A., Guidotti, M., Vitali, A., 2017. Assessing indoor air quality of school environments: transplanted lichen *Pseudovernia furfuracea* as a new tool for biomonitoring and bioaccumulation. *Environ. Monit. Assess.* 189, 358. <https://doi.org/10.1007/s10661-017-6076-2>.
- Roberts, A., Pike, C.R., Verosub, K.L., 2000. First-order reversal curve diagrams: a new tool for characterizing the magnetic properties of natural samples. *J. Geophys. Res.* 105, 28461–28475.
- Roberts, A.P., Heslop, D., Zhao, X., Pike, C.R., 2014. Understanding fine magnetic particle systems through use of first-order reversal curve diagrams. *Rev. Geophys.* 52 (4), 557–602. <https://doi.org/10.1002/2014RG000462>.
- R Core Team, 2022. R: A Language and Environment for Statistical Computing. R Foundation for Statistical Computing, Vienna. <https://www.R-project.org>.
- Roberts, A.P., Almeida, T.P., Church, N.S., Harrison, R.J., Heslop, D., Li, Y., et al., 2017. Resolving the origin of pseudo-single domain magnetic behavior. *J. Geophys. Res. Solid Earth* 122 (12), 9534–9558. <https://doi.org/10.1002/2017JB014860>.
- Sagnotti, L., Macri, P., Egli, R., Mondino, M., 2006. Magnetic properties of atmospheric particulate matter from automatic air sampler stations in Latium (Italy): Toward a definition of magnetic fingerprints for natural and anthropogenic PM10 sources. *J. Geophys. Res.* 111, B12. <https://doi.org/10.1029/2006JB004508>.
- Sagnotti, L., Taddeucci, J., Winkler, A., Cavallo, A., 2009. Compositional, morphological, and hysteresis characterization of magnetic airborne particulate matter in Rome, Italy geochem. *Geophys. Geosyst.* 10 (8) <https://doi.org/10.1029/2009GC002563>.
- Salo, Hanna, 2014. Preliminary comparison of the suitability of three sampling materials to air pollution monitoring. *Fennia* 192 (2), 154–163. ISSN 1798-5617.
- Salo, H., Mäkinen, J., 2019. Comparison of traditional moss bags and synthetic fabric bags in magnetic monitoring of urban air pollution. *Ecol. Indic.* 104, 559–566. <https://doi.org/10.1016/j.ecolind.2019.05.033>.
- Sheikh, H.A., Maher, B.A., Karloukovski, V., Lampronti, G.I., Harrison, R.J., 2022. Biomagnetic characterization of air pollution particulates in Lahore, Pakistan. *Geochem. Geophys. Geosyst.* 23, e2021GC010293 <https://doi.org/10.1029/2021GC010293>. Article.
- Sheikh, H.A., Maher, B.A., Woods, A.W., Tung, P.Y., Harrison, R.J., 2023. Efficacy of green infrastructure in reducing exposure to local, traffic-related sources of airborne particulate matter (PM). *Sci. Total Environ.* 903 <https://doi.org/10.1016/j.scitotenv.2023.166598>.
- Szönyi, M., Sagnotti, L., Hirt, A.M., 2008. A refined biomonitoring study of airborne particulate matter pollution in Rome, with magnetic measurements on quercus ilex tree leaves. *Geophys. J. Int.* 173, 127–141. <https://doi.org/10.1111/j.1365-246X.2008.03715.x>.
- Vannini, A., Paoli, L., Russo, A., Loppi, S., 2019. Contribution of submicronic (PM1) and coarse (PM>1) particulate matter deposition to the heavy metal load of lichens transplanted along a busy road. *Chemosphere* 231, 121–125.
- Winkler, A., Amoroso, A., Di Giosa, A., Marchegiani, G., 2021. The effect of Covid-lockdown on airborne particulate matter in Rome, Italy: a magnetic point of view. *Environ. Pollut.* 291, 118191 <https://doi.org/10.1016/j.envpol.2021.118191>.
- Winkler, A., Contardo, T., Vannini, A., Sorbo, S., Basile, A., Loppi, S., 2020. Magnetic emissions from brake wear are the major source of airborne particulate matter bioaccumulated by lichens exposed in Milan (Italy). *Appl. Sci.* 10, 2073. <https://doi.org/10.3390/app10062073>.
- Winkler, A., Contardo, T., Lapenta, V., Sgamellotti, A., Loppi, S., 2022. Assessing the impact of vehicular particulate matter on cultural heritage by magnetic biomonitoring at Villa Farnesina in Rome, Italy. *Sci. Total Environ.* 823 <https://doi.org/10.1016/j.scitotenv.2022.153729>.